Received: 16 July 2018 | Revised: 27 March 2019 | Accepted: 8 April 2019

DOI: 10.1111/cmi.13031

RESEARCH ARTICLE

WILEY

# *Haemophilus parasuis* infection in 3D4/21 cells induces autophagy through the AMPK pathway

Yijuan Shen | Nini Zhou | Jiahui An | Jiansong Zhang | Meifen Wang | Yufeng Li | Ping Jiang

Key Laboratory of Bacteriology, Ministry of Agriculture, College of Veterinary Medicine, Nanjing Agricultural University, Nanjing, China

**Correspondence**
Yufeng Li, Key Laboratory of Bacteriology, Ministry of Agriculture, College of Veterinary Medicine, Nanjing Agricultural University, Nanjing 210095, China.
Email: yufengli@njau.edu.cn

**Funding information**
Priority Academic Program for Development at Jiangsu Higher Education Institutions (PAPD); National Natural Science Foundation, Grant/Award Number: 31672565; National Key Research and Development Program of China, Grant/Award Number: 2017YFD0500102

## Abstract

*Haemophilus parasuis* (*H. parasuis*) is a common commensal in the upper respiratory tract of pigs, but causes Glässer's disease in stress conditions. To date, many studies focused on the immune evasion and virulence of *H. parasuis*; very few have focused on the role autophagy played in *H. parasuis* infection, particularly in porcine alveolar macrophages (PAMs). In this study, a PAM cell line, 3D4/21 cells were used to study the role of autophagy in *H. parasuis* infection. 3D4/21 cells tandemly expressing GFP, mCherry, and LC3 were infected with *H. parasuis* serovar 5 (*Hps*5). Western blot analysis and confocal and transmission electron microscopy showed that *H. parasuis* infection effectively induces autophagy. Using *Hps* strains of varying virulence (*Hps*4, *Hps*5, and *Hps*7) and UV-inactivated *Hps*5, we demonstrated that autophagy is associated with the internalisation of living virulent strains into cells. In 3D4/21 cells pretreated with rapamycin and 3-MA then infected by *Hps4*, *Hps5*, and *Hps7*, we demonstrated that autophagy affects invasion of *H. parasuis* in cells. AMPK signal results showed that *Hps5* infection can upregulate the phosphorylation level of AMPK, which is consistent with the autophagy development. 3D4/21 cells pretreated with AICAR or Compound C then infected by *Hps*5 revealed that the autophagy induced by *Hps*5 infection is associated with the AMPK pathway. Our study contributes to the theoretical basis for the study of *H. parasuis* pathogenesis and development of novel drugs target for prevention Glässer's disease.

**KEYWORDS**

3D4/21 cells, autophagy, AMPK pathway, *Haemophilus parasuis*

## 1 | INTRODUCTION

*Haemophilus parasuis* (*H. parasuis*), a member of the family *Pasteurellaceae*, is a Gram-negative pleomorphic bacillus and the etiological agent of Glässer's disease, presenting in pigs as polyserositis, polyarthritis, and meningitis (Moller, Andersen, Christensen, & Kilian, 1993). Fifteen standard *H. parasuis* serovars are recognized in addition to non-typeable isolates. Among the standard serovars, 1, 5, 10, 12, 13, and 14 are considered highly virulent, 2, 4, 15, and 8 are mildly virulent, and serovars 3, 6, 7, 9, and 11 are considered avirulent (Rafiee & Blackall, 2000, Del Rio, Gutierrez, & Rodriguez Ferri, 2003). In China, serovars 4 and 5 are the most prevalent, followed by serovars 12, 13, and 14 (Cai et al., 2005; Zhang et al., 2011).

Previous studies have shown that *H. parasuis* infects PUVEC, pig kidney epithelial cells (PK-15), and porcine brain microvascular endothelial cells (Vanier et al., 2006; Zhang et al., 2013). In PK-15 cells,

Yijuan Shen, Nini Zhou, and Jiahui An are equal contributing authors.

  

*H. parasuis* activates NF-κB and MAP kinase signalling pathways mediated by toll-like receptors and the NOD1/2-RIP2 signalling pathway (Chen et al., 2015; Ma et al., 2018). Porcine alveolar macrophages are an important line of defense against *H. parasuis*. During the process of *H. parasuis* infection, PAMs can differentially up-regulate genes related to cytokine production, phagocytosis, phagolysosome formation, signal transduction, and nitric oxide production (Wang et al., 2012). In the lung, the main target of *H. parasuis* infection in pigs, bacteria are in close contact with alveolar macrophages, and their interaction will end in disease development or not. Alexandre et al. have shown that different *H. parasuis* strains isolated from different clinical backgrounds had clear differences in susceptibility to phagocytosis (Olvera, Ballester, Nofrarias, Sibila, & Aragon, 2009). Zeng et al. reported that the rfaD and rfaF genes of *H. parasuis* induce proinflammatory cytokines in PAMs by regulating the NF-κB and MAPKs signalling pathways (Zeng et al., 2018). As is well known, bacterial pathogenicity is the result of the interaction of bacteria and host. Yaning et al. reported that *H. parasuis* infection of PK-15 cells induces TGF-β expression and autophagy, which are associated with the invasion of bacteria (Li, Zhang, Xia, Shen, & Zhang, 2016, Zhang, Li, Yuan, Xia, & Shen, 2016).

Autophagy serves a housekeeping role by removing nonfunctioning proteins and damaged organelles, as well as intracellular pathogens, which has an adaptive role in protecting organisms against diverse pathogens (Cuervo, 2004, Levine & Kroemer, 2008). Autophagy can be induced by hypoxia (Fang, Tan, & Zhang, 2015), nutrient (Steele, Brunton, & Kawula, 2015) or growth factor deprivation (Ni et al., 2014), DNA damage (Houten, Hunter, & Meyer, 2016), or pathogen infection (Steele et al., 2015; Winchell, Steele, Kawula, & Voth, 2015). Previous studies have shown that autophagy plays an important role in the innate immune responses against infection, such as *Mycobacterium tuberculosis* (Mtb) and *Listeria monocytogenes* (Bento, Empadinhas, & Mendes, 2015; Gupta et al., 2015). Conversely, pathogens have evolved strategies to take advantage of autophagy for infection, replication, and survival (Dorn, Dunn, & Progulske-Fox, 2002, Campoy & Colombo, 2009, Castrejon-Jimenez, Leyva-Paredes, Hernandez-Gonzalez, Luna-Herrera, & Garcia-Perez, 2015). 3-MA, a PtdIns3K inhibitor that effectively blocks an early stage of autophagy by inhibiting the class III PtdIns3K, but not a specific autophagy inhibitor. Rapamycin binds to FKBP1A/FKBP12 and inhibits MTORC1, which can bind to the FRB domain of MTOR and limits its interaction with RPTOR and induce autophagy, but only providing partial MTORC1 inhibition (Klionsky et al., 2016). 3-MA and rapamycin were often used as negative and positive controls in autophagy study. Autophagy is associated with the AMPK, Erk, MAPK, and p53 signal pathways. AMP-activated protein kinase (AMPK) is an energy sensor activated by an increase in the ratio of AMP/ATP or glucose starvation, which leads to TSC2 phosphorylation and suppresses mTOR and activates autophagy (Hardie, 2011; Li, Huang, Lu, & Luo, 2015). AMPK is a heterotrimeric complex consisting of an α-catalytic subunit, a β-regulatory subunit, and a γ-regulatory subunit. AMPK activity is increased when its Thr172 residue (α subunit) is phosphorylated by upstream kinases (Zhang et al., 2016). Although existing studies suggest that AMPK is closely involved in the induction of autophagy, it is not clear whether autophagy induced by *H. parasuis* is associated with the AMPK pathway. In this study, we observed that *H. parasuis* induces autophagy in 3D4/21 cells and that autophagy is associated with *Hps* virulence, and invasion, and the AMPK pathway.

## 2 | MATERIAL AND METHODS

### 2.1 | Regents

Rabbit polyclonal antibody against LC3B was obtained from Sigma-Aldrich. Rabbit polyclonal antibody against AMPKα1 and phospho-AMPKα (Thr172) (40H9) was obtained from Cell Signaling Technology, and β-actin antibody was obtained from Santa Cruz Biotechnology. Recombinant adenovirus tandem expressing mCherry-GFP-LC3 was purchased from HANBIO. RIPA lysis buffer, HRP-labelled goat anti-rabbit IgG (H + L), HRP-labelled goat anti-mouse IgG (H + L), and rabbit polyclonal antibody against GFP were purchased from Beyotime Biosciences. ECL substrate was purchased from Thermo Fisher Scientific. 3-Methyladenine and rapamycin were purchased from Sigma. AICAR (5-aminoimidazole-4-carboxamide ribonucleotide) and Compound C were purchased from R&D.

### 2.2 | Bacterial strains and culture conditions

*Hps*5 (highly virulent), *Hps*4 (moderately virulent), and *Hps*7 (avirulent) were used in this study. Bacteria were cultured at 37°C on Trypticase Soy Agar and in Trypticase Soy Broth (TSA and TSB, respectively; OXOID) supplemented with 0.01% nicotinamide adenine dinucleotide (NAD) and 5% (v/v) inactivated bovine serum. Bacteria were grown overnight in TSB at 37°C and 200 rpm; before use, bacteria were diluted 1:100 in fresh medium and incubated as above until $OD_{600}$ reached 0.6.

### 2.3 | 3D4/21 cell culture

3D4/21 cells were grown in RPMI 1640 (Invitrogen) supplemented with 10% heat-inactivated fetal bovine serum (FBS, Invitrogen), 100 U/ml of penicillin G (Invitrogen), 100 mg/ml of streptomycin (Invitrogen), and MEM non-essential amino acids (Invitrogen). Cells were cultured in a humidified atmosphere at 37°C with 5% $CO_2$. Cells were subcultured upon reaching 90% confluence.

### 2.4 | Bacterial infection

3D4/21 cells ($3 \times 10^5$ cells/well) were seeded into 24 well plates. At 50% confluence, cells were inoculated with 10 moi of adenovirus tandemly expressing GFP, mCherry, and LC3. After 36 hr, cells were washed with sterile PBS and then inoculated with different serovars of *H. parasuis* at different mois. The plates were centrifuged at 800 *g* for 10 min and incubated at 37°C in 5% $CO_2$. After 1 hr, cells were harvested by scraping, transferred to sterile centrifuge tubes, and

centrifuged for 1 min at 12,000 *g*. Supernatants were discarded, and pellets were resuspended in an equal volume of PBS. The resuspended cells were smeared onto Trypticase Soy Agar plates and incubated at 37°C for 48 hr.

### 2.5 | Adherence and invasion assays

Cells ($3 \times 10^5$ cells/well) were seeded into 24-well tissue culture plates. Prior to infection, cells were washed with sterile PBS to remove antibiotics and then inoculated with *Hps4*, *Hps5*, and *Hps7* at a moi of 10. Plates were centrifuged at 800 *g* for 10 min and incubated at 37°C in 5% $CO_2$. The cells were incubated 1 and 2 hr for adherence and invasion, respectively, and then vigorously washed five times with PBS to remove nonspecifically attached bacteria. For invasion assay, complete growth medium (including 100 U/ml of penicillin G and 0.25 mg/ml of gentamicin) was added to each well, and plates were incubated for additional 1 hr to kill extracellular *H. parasuis* and washed five times with PBS and incubate for additional 0, 1, 3, and 5 hr, respectively. The above cells were incubated 10 min at 37°C with 100 μl of 0.025% trypsin. Following trypsin treatment, cells were collected by centrifugation as described above. At the same time, cells were prior treated with Rapa and 3-MA and infected with *Hps4*, *Hps5*, and *Hps7*, and adherence and invasion were performed as above mentioned.

### 2.6 | Western blot

Cells grown in 24-well plates were incubated with 5 μM of rapamycin for 12 hr and 2 mM of 3-MA for 4 hr and infected with *Hps*5, *Hps4*, and *Hps7* at 10 moi, or mock infected with an equal amount of PBS and incubated at 37°C in 5% $CO_2$. The treated cells were lysed in RIPA lysis and centrifuged at 13 000 rpm for 25 min at 4°C, and supernatants were boiled with 5× loading buffer and separated by 10% SDS-PAGE and transferred to NC membranes. Membranes were blocked with 10% skim milk at room temperature for 2 hr and then incubated with specific antibodies (1μg/ml) at 4°C overnight. Membranes were rinsed five times with PBST and then incubated with HRP-labelled goat anti-rabbit IgG (H + L) and HRP-labelled goat anti-mouse IgG (H + L; 1:10,000 dilution) at 4°C for 1 hr. The membranes were incubated with ECL reagent, and the signal was analysed by a Quantity System Image Analyser.

### 2.7 | Confocal microscopy

Cells grown on coverslips in 24-well plates were incubated with 5 μM of rapamycin for 12 hr and 2 mM of 3-MA for 4 hr, or left untreated and then infected with *Hps*5, *Hps4*, and *Hps7* at 10 moi, or mock infected with an equal amount of PBS and incubated 37°C in 5% $CO_2$. After 6 hr incubation, coverslips were washed with sterile PBS to remove nonspecifically attached bacteria, and cells were fixed with acetone and methanol (1:1) for 30 min. Coverslips were mounted on microscope slides, and cells were viewed using a Zeiss LSM 700 confocal microscope.

### 2.8 | Transmission electron microscopy (TEM)

Cells prepared for TEM were treated with drugs and infected with *Hps*5 or mock infected as described above. Cells were washed with sterile PBS to remove nonspecifically attached bacteria, harvested using a cell scraper, and centrifuging 300 *g* for 10 min at 4°C. Supernatants were discarded, and the cells were fixed with 2.5% glutaraldehyde at 4°C for 12 hr and observed with a transmission electron microscope.

### 2.9 | Statistics

Three biological replicates were carried out for every experiment, and results were recorded as mean value ± *SD*. GraphPad Prism 5 was used to analyse differences between groups (one-way ANOVA; Tukey's post hoc test, $^{***}P < .001$, $^{**}P < .01$, $^{*}P < .05$). ImageJ software was used to quantify the western blot bands. Results are normalised to the β-actin in each sample.

## 3 | RESULTS

### 3.1 | *H. parasuis* infection induces autophagy

To determine whether infection by *H. parasuis* can induce autophagy, 3D4/21 cells were infected with adenovirus tandemly expressing mCherry-GFP-LC3. After confirming the expression of mCherry-GFP-LC3, the cells were treated with rapamycin, 3-MA, or infected with various moi of *Hps5* for 2, 4, and 6 hr. As seen in Figure S1, mCherry-GFP-LC3-II levels in *Hps*5-infected cells were decreased at

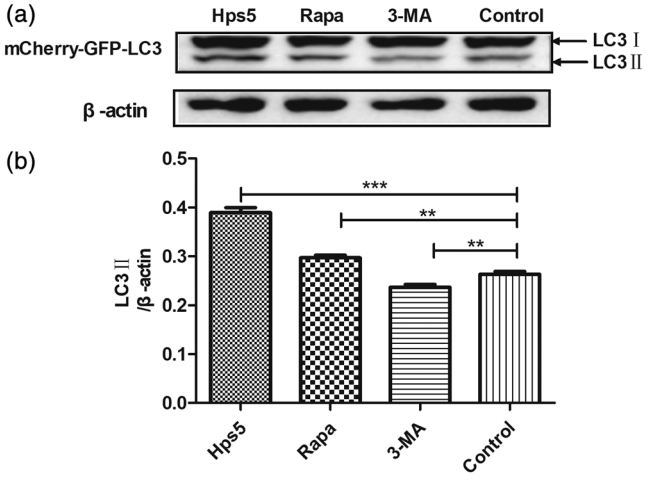


**FIGURE 1** Western blot of LC3-II expression in 3D4/21 cells. (a) mCherry-GFP-LC3 expression in untreated, rapamycin-treated, 3-MA-treated cells and infected by *Hps*5 at moi 10 and incubated for 6 hr. (b) The ratio of LC3-II/β-actin (one-way ANOVA; Dunnett's multiple comparison test, $^{***}P < .001$, $^{**}P < .01$)

2 and 4 hr post infection compared with mock-infected controls. By 6 h post infection, the level of mCherry-GFP-LC3-II had significantly increased over mock-infected controls ($P < .001$). As seen in Figure S2, the levels of LC3-II were nearly equal in cells infected with 100 or 10 moi for 6 hr, which has significant difference than that of 1 and 0.1 moi. After optimization, the conditions of *Hps5* infection using 10 moi and incubation for 6 hr were used in all experiments, which can induce significant autophagy (Figure 1).

Confocal microscopy of these cells (Figure 2) revealed more puncta associated with autophagy were observed in rapamycin-treated (positive control) and *Hps5*-infected cells, than in *Hps4*-, *Hps7*-, and 3-MA treated cells (negative control) at 6 hr. These results are consistent with the expression of LC3-II seen in the western blots. Importantly, there were more significantly red and yellow puncta in *Hps5*-infected cells than in *Hps4*, *Hps7*, and control cells, which further confirmed the induction of autolysosome formation (Figure 2b). Taken together, above findings further confirmed that the infection by highly virulent *Hps5* can specifically induce autophagy in 3D4/21 cells. Especially, we found autophagy formation is related with the virulence of *H. parasuis*.

Transmission electron microscopy revealed that autophagosomes, double-membrane structures containing heterogeneous material, were readily apparent in cells infected by *Hps*5 or treated with rapamycin (Figure 3c,d, respectively). None were observed in the negative controls and 3-MA-treated cells (Figure 3a,b, respectively). These results demonstrate that *Hps*5 infection effectively induces autophagy in 3D4/21 cells.

## 3.2 | Autophagy is associated with internalisation of virulent strains into cells

3D4/21 cells were infected at moi 10 with *Hps*5, *Hps*4, and *Hps*7 for 6 hr. The adherence and invasion assay showed that *Hps7* has the highest adherence capacity at 1 hr, which followed by *Hps4* and *Hps5* in turn. At 3 hr, *Hps7* and *Hps4* enter into cells higher than that of *Hps5*, but they decreased more rapidly than *Hps5* from 4 to 8 hr. At 6 hr, we found more *Hps5* in the cells (Figure 4). The greatest level of autophagy was induced by *Hps*5 infection, and the less virulent strains induced correspondingly lower levels of autophagy (Figure 5a). As seen in Figure 5b, the autophagy induced by living *Hps*5 is significantly higher than that of induced by UV-inactivated *Hps*5. We conclude that the autophagy induced by *H. parasuis* is positively related with the internalisation of living virulent *H. parasuis* strains into cells, which is not simply associated with bacteria load into cells.

## 3.3 | Autophagy affects invasion of *H. parasuis* into 3D4/21 cells

The bacterial adherence and invasion assay were performed as described with 3D4/21 that had been treated with 5 μM of rapamycin and 2 mM of 3-MA, or mock treated, and then infected with *Hps4*, *Hps*5, and *Hps*7 at moi 10 for 1 and 3 hr. As is shown in Figure 6, the CFUs of *H. parasuis* in rapamycin-treated cells is significantly lower

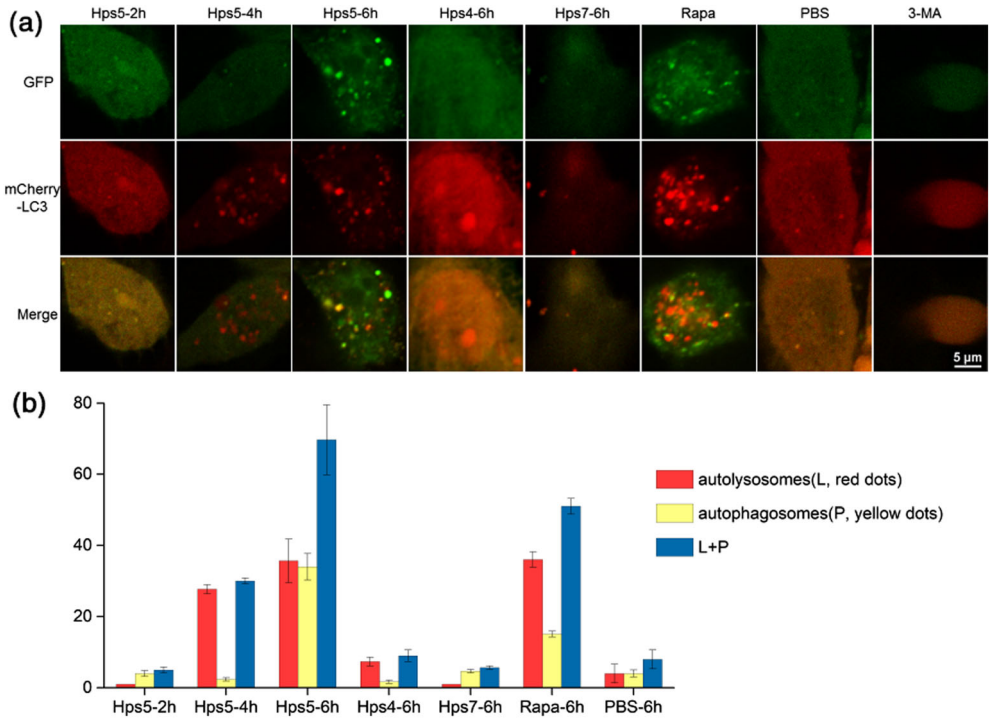


**FIGURE 2** *H. parasuis* infection induced autophagy. (a) Confocal microscopy. PBS: cells were treated with PBS; *Hps4*, *Hps*5, and *Hps7*: cells infected with 10 moi *Hps4*, *Hps5*, *and Hps7* for 6 hr; Rapa: cells treated with 5 μM of rapamycin for 12 hr; 3-MA: cells treated with 2 mM 3-MA for 4 hr. (b) Puncta numbers in each cell were analysed. The data are representative of 10 cells for each channel (one-way ANOVA; Dunnett's multiple comparison test, $^{***}P < .001$, $^{**}P < .01$)

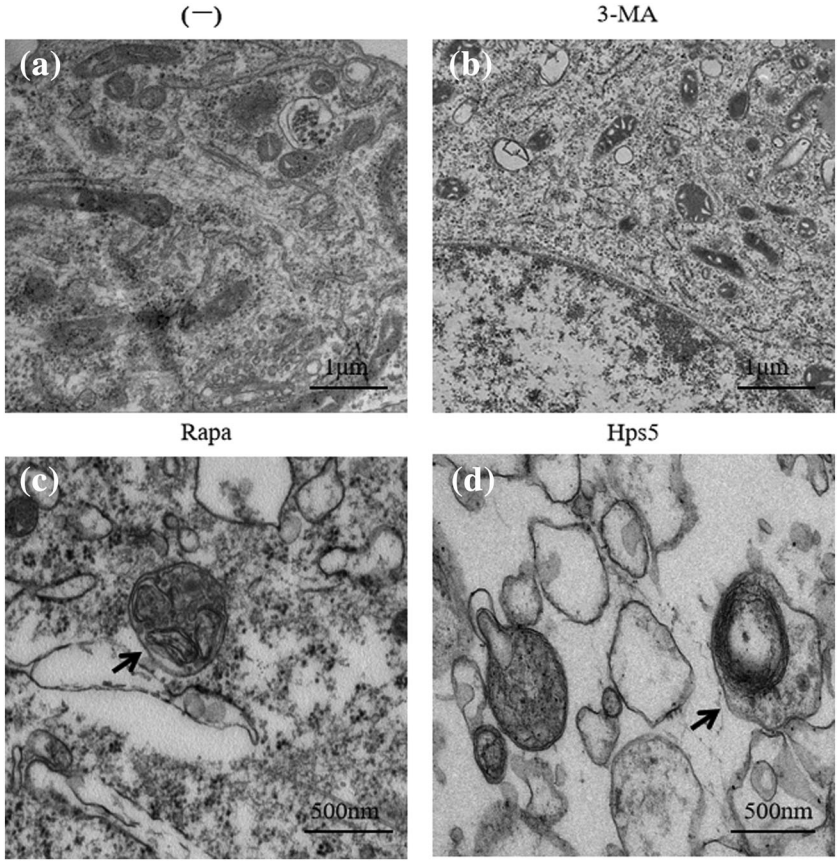


**FIGURE 3** Transmission electron microscope. (-): Untreated/uninfected cells; *Hps5*: cells treated with 10 moi of *Hps*5 for 6 hr; 3-MA: cells treated with 2 mM of 3-MA for 4 hr; Rapa: cells treated with 5 μM of rapamycin for 12 hr

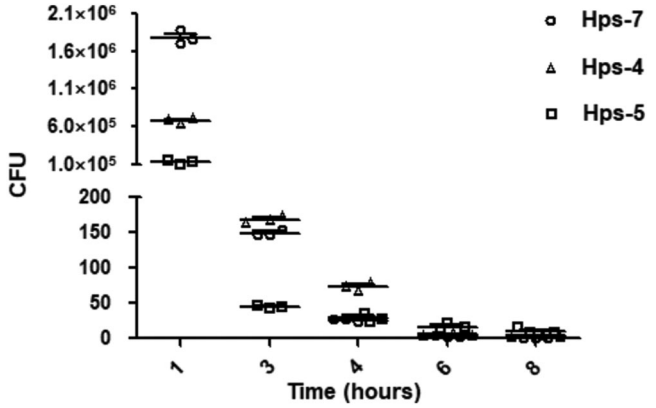


**FIGURE 4** Adherence and invasion assays of different virulent *H. parasuis* strains. 3D4/21 cells were infected with avirulent *Hps7*, medium virulent *Hps4*, and highly virulent *Hps5* at 10 moi. The samples were collected at 1, 3, 4, 6, and 8 hr and smeared onto TSA plates and CFU were counted

than that of the untreated control cells, demonstrating that autophagy induced by rapamycin affects invasion of *H. parasuis* in 3D4/21 cells.

### 3.4 | *H. parasuis* infection activates AMPK pathway

3D4/21 cells were infected with *Hps5* at a moi of 10 and collected at 2, 4, and 6 hr, respectively. Western blot results (Figure 7) showed that the ratio of p-AMPK/AMPK increased from 2 hr and steadily increased from 4 to 6 hr and peaked at 6 hr, which indicated that *Hps5* infection can effectively activate AMPK signal pathway.

### 3.5 | AMPK signal is associated with *H. parasuis* invasion

AICAR, AMP-mimetic 5-aminoimidazole-4-carboxamide-1-β-D-ribofuranoside, which can permeate cell membrane and activate AMPK signal pathway. Compound C is an effective and antiselective AMPK inhibitors. 3D4/21 cells were, respectively, treated with 0.5 mM of AICAR and 0.5 μM of Compound C for 24 hr, or left untreated, and then infected with *Hps*5 at moi 10 for 3 hr. The western blots showed that the ratio of p-AMPK/AMPK was increased in AICAR-treated cells compared with untreated and decreased in Compound C-treated cells compared with untreated (Figures 8a and 9a). At the same time, we found AICAR and Compound C treatment can induce and inhibit autophagy, respectively (Figures 8b and 9b). The invasion assay results showed that the number of *H. parasuis* internalised in AICAR-treated cells is significantly lower than the *H. parasuis* internalised in untreated cells (Figure 8c). The number of *H. parasuis* in Compound C-treated cells is significantly higher than that in untreated cells (Figure 9c). These results further support that autophagy induced by *H. parasuis* infection is associated with the AMPK pathway.

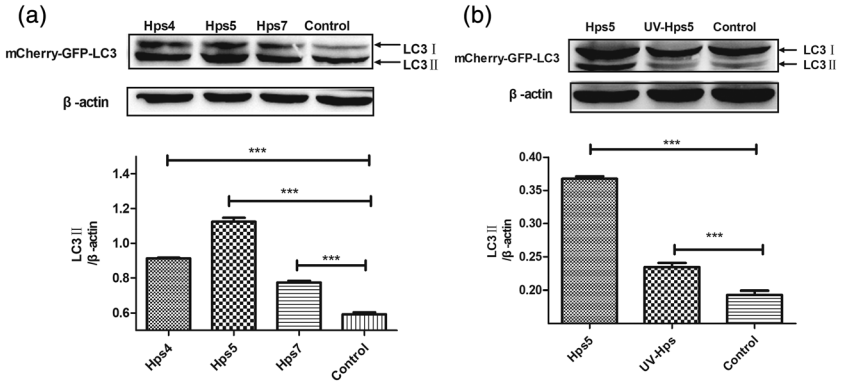


**FIGURE 5** Western blots of GFP-RFP-LC3 expression in 3D4/21 cells. (a) Cells infected with *Hps*4, *Hps*5, and *Hps*7 or mock infected. (b) Cells infected with *Hps*5, UV-inactivated *Hps*5, or mock infected. The ratio of LC3-II/β-actin for each treatment is depicted in the bar graph below the corresponding western blot (one-way ANOVA; Dunnett's multiple comparison test, $^{***}P < .001$).

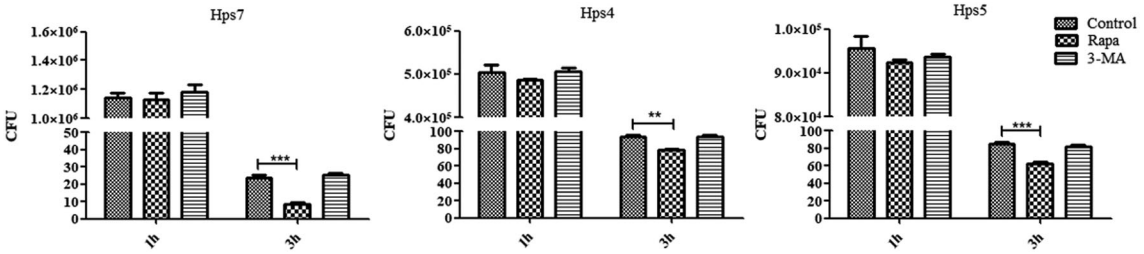


**FIGURE 6** Number of internalized CFU in *Hps*4-, *Hps*5-, *and Hps*7-infected cells that were pretreated with rapamycin, 3-MA, or untreated (one-way ANOVA; Dunnett's multiple comparison test, $^{*}P < .05$)

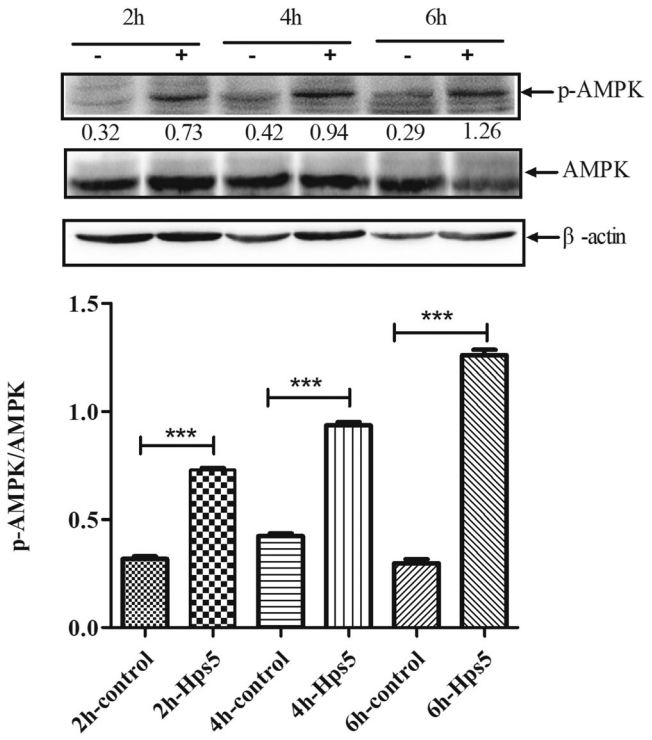


**FIGURE 7** Western blot of the time course of p-AMPK expression in 3D4/21 cells infected with *Hps*5. The ratio of p-AMPK/AMPK for each experiment is depicted in the graph below the corresponding western blot

## 4 | DISCUSSION

Glässer's disease is caused by *H. parasuis*, a bacterium widely distributed in swine herds, and causes large economic costs to swine industries throughout the world. Most studies of *H. parasuis* pathogenesis have focused on the bacterial virulence factors, such as cytolethal distending toxin, capsule, virulence-associated trimeric autotransporters, and the outer membrane proteins (Costa-Hurtado & Aragon, 2013).

As is well known to all that autophagy plays important roles in the interaction between host and bacteria, we want to know the roles that autophagy played in the interaction between 3D4/21 cells and *H. parasuis*. Confocal microscopy, western blot, and transmission electron microscopy showed that *H. parasuis* infection effectively induces autophagy in 3D4/21 cells. Results from infections with UV-inactivated *Hps5* and stains of varying virulence showed that autophagy is positively associated with the internalisation of virulent *H. parasuis* into cells. These observations showed that only cellular virulent bacteria can effectively induce autophagy in 3D4/21 cells and double membrane autophagosome were observed in electronical microscopic view. More significant red puncta associated with autophagy were found in the cells infected by *Hps5* than that by *Hps4* and *Hps7*, which further confirmed that autophagy is positively related with the virulence of *H. parasuis*, but not to the blockage of autophagic flux. Treatment of 3D4/21 cells with rapamycin prior to infection by

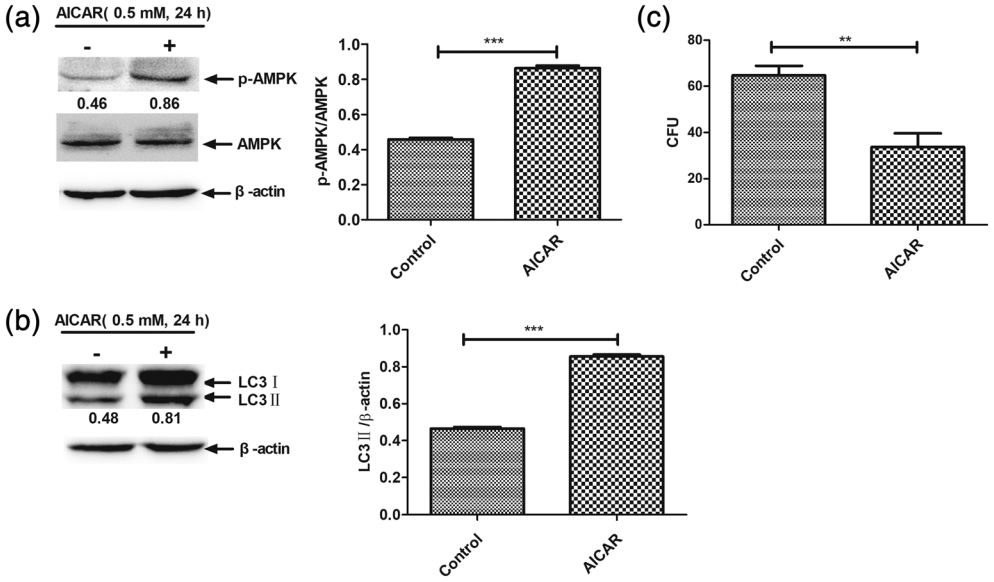


**FIGURE 8** Western blot of 3D4/21 cells treated with AICAR or untreated and infected by *Hps*5. The difference grey of p-AMPK and LC3 II was standardized with the AMPK and β-actin, respectively. CFU of internalised bacteria is illustrated in the bar graph below the corresponding western blot (*t* test; paired *t* test, $^{**}P < .01$). (a) p-AMPK expression after treated with AICAR; (b) LC3 II expression after treated with AICAR; (c) The internalised CFUs after treated with AICAR

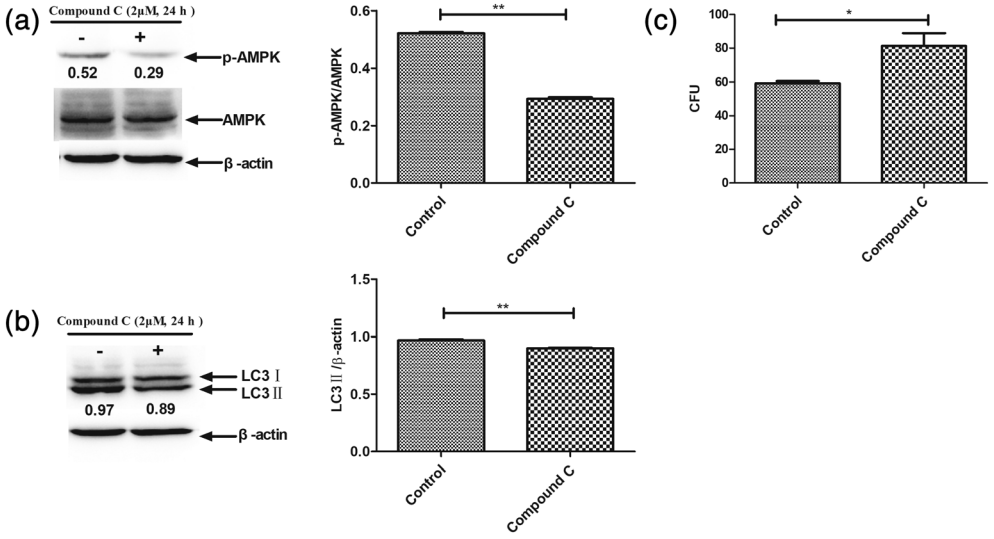


**FIGURE 9** Western blot of 3D4/21 cells treated with Compound C or untreated and infected by *Hps*5. The difference grey of p-AMPK and LC3 II were standardised with AMPK and β-actin. CFU of internalised bacteria are illustrated in the bar graph below the corresponding western blot (*t* test; paired *t* test, $^{**}P < .01$). (a) p-AMPK expression after treated with Compound C; (b) LC3 II expression after treated with Compound C; (c) The internalised CFUs after treated with Compound C

*H. parasuis* demonstrated that autophagy can inhibit the invasion of bacteria into cells; this is consistent with previous reports (Zhang, Li, et al., 2016). We found that *H. parasuis* infection inhibits autophagy early in infection (2–4 hr), but this effect diminishes at later times in infection (6 hr). This suggests an arms race maybe existed between *H. parasuis* and host. This phenomenon was also found in human cytomegalovirus (HCMV) infection (Chaumorcel, Souquere, Pierron, Codogno, & Esclatine, 2008).

A growing body of evidence has shown that the AMPK pathway plays an important role in autophagy. Yang et al. have shown that AMPK activation by AICAR enhances autophagy and the antimicrobial response against intracellular mycobacterial infection (Yang et al., 2014). Based on the known role of the AMPK pathway in autophagy, we investigated the AMPK-mediated activation of autophagy in PAM cells infected with *H. parasuis*. We found that *Hps5* infection increased the level of p-AMPK at 2, 4, and 6 hr, and there is a little different

from autophagy development at 2 and 4 hr, but which is consistent with autophagy development at 6 hr. This may be explained by the lag behind of autophagy development after the activation of AMPK signal pathway. So we can conclude that *Hps5* infection can activate AMPK signal pathway.

In order to further confirm the relationship between *Hps5* infection and AMPK signal pathway, the AMPK activator AICAR and inhibitor Compound C were used to activate and inhibit the AMPK pathway in cells that were then infected by *H. parasuis*. The CFU results showed that the phosphorylation of AMPK and autophagy are negatively associated with the invasion of bacteria in 3D4/21 cells, which further confirms that autophagy plays an important role in clearing bacteria from cells.

## 5 | CONCLUSION

3D4/21 cells, a porcine alveolar macrophage cell line, were used to study autophagy induced by *H. parasuis* infection. We found *H. parasuis* infection effectively induces autophagy in these cells and is positively associated with the internalisation of virulent *H. parasuis* via the AMPK pathway.

### ACKNOWLEDGEMENTS

This study was supported by the National Key Research and Development Program of China (2017YFD0500102), National Natural Science Foundation (31672565), and the Priority Academic Program for Development at Jiangsu Higher Education Institutions (PAPD).

### CONFLICTS OF INTEREST

None of the authors has any financial or personal relationships that could inappropriately influence or bias the content of the paper.

### ORCID

*Yufeng Li* https://orcid.org/0000-0003-2181-6319

### REFERENCES

Bento, C. F., Empadinhas, N., & Mendes, V. (2015). Autophagy in the fight against tuberculosis. *DNA and Cell Biology*, *34*, 228–242. https://doi.org/10.1089/dna.2014.2745

Cai, X., Chen, H., Blackall, P. J., Yin, Z., Wang, L., Liu, Z., & Jin, M. (2005). Serological characterization of *Haemophilus parasuis* isolates from China. *Veterinary Microbiology*, *111*, 231–236. https://doi.org/10.1016/j.vetmic.2005.07.007

Campoy, E., & Colombo, M. I. (2009). Autophagy in intracellular bacterial infection. *Biochimica et Biophysica Acta*, *1793*, 1465–1477. https://doi.org/10.1016/j.bbamcr.2009.03.003

Castrejon-Jimenez, N. S., Leyva-Paredes, K., Hernandez-Gonzalez, J. C., Luna-Herrera, J., & Garcia-Perez, B. E. (2015). The role of autophagy in bacterial infections. *Bioscience Trends*, *9*, 149–159. https://doi.org/10.5582/bst.2015.01035

Chaumorcel, M., Souquere, S., Pierron, G., Codogno, P., & Esclatine, A. (2008). Human cytomegalovirus controls a new autophagy-dependent cellular antiviral defense mechanism. *Autophagy*, *4*, 46–53. https://doi.org/10.4161/auto.5184

Chen, Y., Liu, T., Langford, P., Hua, K., Zhou, S., Zhai, Y., … Zhou, R. (2015). *Haemophilus parasuis* induces activation of NF-kappaB and MAP kinase signaling pathways mediated by toll-like receptors. *Molecular Immunology*, *65*, 360–366. https://doi.org/10.1016/j.molimm.2015.02.016

Costa-Hurtado, M., & Aragon, V. (2013). Advances in the quest for virulence factors of *Haemophilus parasuis*. *Veterinary Journal*, *198*, 571–576. https://doi.org/10.1016/j.tvjl.2013.08.027

Cuervo, A. M. (2004). Autophagy: In sickness and in health. *Trends in Cell Biology*, *14*, 70–77. https://doi.org/10.1016/j.tcb.2003.12.002

Del Rio, M. L., Gutierrez, C. B., & Rodriguez Ferri, E. F. (2003). Value of indirect hemagglutination and coagglutination tests for serotyping *Haemophilus parasuis*. *Journal of Clinical Microbiology*, *41*, 880–882.

Dorn, B. R., Dunn, W. A. Jr., & Progulske-Fox, A. (2002). Bacterial interactions with the autophagic pathway. *Cellular Microbiology*, *4*, 1–10. https://doi.org/10.1046/j.1462-5822.2002.00164.x

Fang, Y., Tan, J., & Zhang, Q. (2015). Signaling pathways and mechanisms of hypoxia-induced autophagy in the animal cells. *Cell Biology International*, *39*, 891–898. https://doi.org/10.1002/cbin.10463

Gupta, M., Shin, D. M., Ramakrishna, L., Goussetis, D. J., Platanias, L. C., Xiong, H., … Ozato, K. (2015). IRF8 directs stress-induced autophagy in macrophages and promotes clearance of *Listeria monocytogenes*. *Nature Communications*, *6*, 6379. https://doi.org/10.1038/ncomms7379

Hardie, D. G. (2011). AMPK and autophagy get connected. *The EMBO Journal*, *30*, 634–635. https://doi.org/10.1038/emboj.2011.12

Houten, B. V., Hunter, S. E., & Meyer, J. N. (2016). Mitochondrial DNA damage induced autophagy, cell death, and disease. *Frontiers in Bioscience*, *21*, 42–54. https://doi.org/10.2741/4375

Klionsky, D. J., Abdelmohsen, K., Abe, A., Abedin, M. J., Abeliovich, H., Acevedo Arozena, A., … Zughaier, S. M. (2016). Guidelines for the use and interpretation of assays for monitoring autophagy (3rd edition). *Autophagy*, *12*, 1–222. https://doi.org/10.1080/15548627.2015.1100356

Levine, B., & Kroemer, G. (2008). Autophagy in the pathogenesis of disease. *Cell*, *132*, 27–42. https://doi.org/10.1016/j.cell.2007.12.018

Li, N., Huang, D., Lu, N., & Luo, L. (2015). Role of the LKB1/AMPK pathway in tumor invasion and metastasis of cancer cells (Review). *Oncology Reports*, *34*, 2821–2826. https://doi.org/10.3892/or.2015.4288

Li, Y., Zhang, Y., Xia, Y., Shen, Y., & Zhang, J. (2016). *Haemophilus parasuis* modulates cellular invasion via TGF-beta1 signaling. *Veterinary Microbiology*, *196*, 18–22. https://doi.org/10.1016/j.vetmic.2016.10.012

Ma, B., Hua, K., Zhou, S., Zhou, H., Chen, Y., Luo, R., … Jin, H. (2018). *Haemophilus parasuis* infection activates NOD1/2-RIP2 signaling pathway in PK-15 cells. *Developmental and Comparative Immunology*, *79*, 158–165. https://doi.org/10.1016/j.dci.2017.10.021

Moller, K., Andersen, L. V., Christensen, G., & Kilian, M. (1993). Optimalization of the detection of NAD dependent *Pasteurellaceae* from the respiratory tract of slaughterhouse pigs. *Veterinary Microbiology*, *36*, 261–271. https://doi.org/10.1016/0378-1135(93)90093-M

Ni, B. B., Li, B., Yang, Y. H., Chen, J. W., Chen, K., Jiang, S. D., & Jiang, L. S. (2014). The effect of transforming growth factor beta1 on the crosstalk between autophagy and apoptosis in the annulus fibrosus cells under serum deprivation. *Cytokine*, *70*, 87–96. https://doi.org/10.1016/j.cyto.2014.07.249

Olvera, A., Ballester, M., Nofrarias, M., Sibila, M., & Aragon, V. (2009). Differences in phagocytosis susceptibility in *Haemophilus parasuis* strains. *Veterinary Research*, *40*, 24. https://doi.org/10.1051/vetres/2009007

Rafiee, M., & Blackall, P. J. (2000). Establishment, validation and use of the Kielstein-Rapp-Gabrielson serotyping scheme for *Haemophilus parasuis*. *Australian Veterinary Journal*, *78*, 172–174. https://doi.org/10.1111/j.1751-0813.2000.tb10586.x

Steele, S., Brunton, J., & Kawula, T. (2015). The role of autophagy in intracellular pathogen nutrient acquisition. *Frontiers in Cellular and Infection Microbiology*, *5*, 51. https://doi.org/10.3389/fcimb.2015.00051

Vanier, G., Szczotka, A., Friedl, P., Lacouture, S., Jacques, M., & Gottschalk, M. (2006). *Haemophilus parasuis* invades porcine brain microvascular endothelial cells. *Microbiology*, *152*, 135–142. https://doi.org/10.1099/mic.0.28312-0

Wang, Y., Liu, C., Fang, Y., Liu, X., Li, W., Liu, S., … He, Q. (2012). Transcription analysis on response of porcine alveolar macrophages to *Haemophilus parasuis*. *BMC Genomics*, *13*, 68. https://doi.org/10.1186/1471-2164-13-68

Winchell, C. G., Steele, S., Kawula, T., & Voth, D. E. (2015). Dining in: Intracellular bacterial pathogen interplay with autophagy. *Current Opinion in Microbiology*, *29*, 9–14. https://doi.org/10.1016/j.mib.2015.09.004

Yang, C. S., Kim, J. J., Lee, H. M., Jin, H. S., Lee, S. H., Park, J. H., … Jo, E. K. (2014). The AMPK-PPARGC1A pathway is required for antimicrobial host defense through activation of autophagy. *Autophagy*, *10*, 785–802. https://doi.org/10.4161/auto.28072

Zeng, Z., Chen, X., Yue, H., He, H., Ren, Y., Tang, C., & Zhang, B. (2018). The effect of rfaD and rfaF of *Haemophilus parasuis* on lipooligosaccharide induced inflammation by NF-kappaB/MAPKs signaling in porcine alveolar macrophages. *The Journal of veterinary medical science/the Japanese Society of Veterinary Science*, *80*, 842–845. https://doi.org/10.1292/jvms.16-0586

Zhang, B., Xu, C., Zhang, L., Zhou, S., Feng, S., He, Y., & Liao, M. (2013). Enhanced adherence to and invasion of PUVEC and PK-15 cells due to the overexpression of RfaD, ThyA and Mip in the DeltaompP2 mutant of *Haemophilus parasuis* SC096 strain. *Veterinary Microbiology*, *162*, 713–723. https://doi.org/10.1016/j.vetmic.2012.09.021

Zhang, D., Wang, W., Sun, X., Xu, D., Wang, C., Zhang, Q., … Liu, Z. (2016). AMPK regulates autophagy by phosphorylating BECN1 at threonine 388. *Autophagy*, *12*, 1447–1459. https://doi.org/10.1080/15548627.2016.1185576

Zhang, J., Xu, C., Guo, L., Ke, B., Ke, C., Zhang, B., … Liao, M. (2011). A rapid pulsed-field gel electrophoresis method of genotyping *Haemophilus parasuis* isolates. *Letters in Applied Microbiology*, *52*, 589–595. https://doi.org/10.1111/j.1472-765X.2011.03048.x

Zhang, Y., Li, Y., Yuan, W., Xia, Y., & Shen, Y. (2016). Autophagy is associated with pathogenesis of *Haemophilus parasuis*. *Frontiers in Microbiology*, *7*, 1423. https://doi.org/10.3389/fmicb.2016.01423

## SUPPORTING INFORMATION

Additional supporting information may be found online in the Supporting Information section at the end of the article.

**How to cite this article:** Shen Y, Zhou N, An J, et al. *Haemophilus parasuis* infection in 3D4/21 cells induces autophagy through the AMPK pathway. *Cellular Microbiology*. 2019;21:e13031. https://doi.org/10.1111/cmi.13031